Monatshefte für Chemie 112, 317—333 (1981)

Monatshefte für Chemie

Self-Consistent APW Band Structure Calculations for the Intermetallic Compounds FeAl, CoAl, and NiAl

Karl Pechter[a], **Peter Rastl**[a], **Adolf Neckel**[b,*], **Renate Eibler**[b], and **Karlheinz Schwarz**[c]

[a] Interfakultäres Rechenzentrum, Universität Wien, A-1010 Wien, Austria

[b] Institut für Physikalische Chemie, Universität Wien, A-1090 Wien, Austria

[c] Institut für Technische Elektrochemie, Technische Universität Wien, A-1060 Wien, Austria

(Received 21 October 1980. Accepted 27 November 1980)

Self-consistent augmented plane wave (APW) band structure calculations have been performed for the compounds FeAl, CoAl, and NiAl. For CoAl as a representative example the following results are presented: energy eigenvalues, band structure, radial charge densities and charge transfer. The charge distribution for all three compounds is displayed in tabular form and sections through the *Fermi* surface are shown. The results are compared with previous band structure calculations on these substances. Reference is made to papers which have used the present results to calculate several physical properties of the investigated compounds.

(Keywords: Band structure; Charge distribution; CoAl; FeAl; NiAl)

Selbstkonsistente Bandstrukturrechnungen für die intermetallischen Verbindungen FeAl, CoAl *und* NiAl

Für die Verbindungen FeAl, CoAl und NiAl wurden selbstkonsistente APW (augmented plane wave) Bandstrukturrechnungen durchgeführt. Energieeigenwerte, Bandstruktur, radiale Ladungsdichten und Ladungsüberführung werden für CoAl als repräsentatives Beispiel angegeben. Für alle drei Verbindungen wird die Ladungsverteilung in Tabellenform dargestellt, und es werden Schnitte durch die *Fermi*oberfläche gezeigt. Die Ergebnisse dieser Arbeit werden mit den Resultaten früherer Berechnungen verglichen. Ferner wird auf Arbeiten hingewiesen, in welchen auf Grundlage der vorliegenden Bandstrukturrechnungen verschiedene physikalische Eigenschaften der genannten Verbindungen ermittelt wurden.

0026-9247/81/0112/0317/$ 03.40

Introduction

In this paper APW band structure calculations are presented for the ordered stoichiometric compounds FeAl, CoAl, and NiAl. These compounds have been selected for a theoretical investigation, because various experimental data concerning their electronic structure are available. Furthermore, band structure calculations of ordered intermetallic compounds may serve as a starting point for studies of substitutional disordered alloys. Due to these facts and because of their simple CsCl type crystal structure these substances have already received considerable theoretical attention in literature.

Hume-Rothery[1] suggested that NiAl and CoAl are electron compounds formed at an electron to atom ratio of 3/2, where only the valence electrons of aluminium are taken into account. The first rigorous band structure calculation on one of these compounds (NiAl) was performed by *Connolly* and *Johnson*[2], who used the non self-consistent APW and KKR method. *Moruzzi*, *Williams* and *Janak*[3] studied the band narrowing and the charge transfer in CoAl, NiAl and four other intermetallic compounds, crystallizing with the CsCl type structure, by means of the self-consistent KKR method. The electronic band structure of FeAl was computed by *Okochi*[4] via the non self-consistent APW method. *Nagel* et al.[5] investigated the electronic structure of FeAl, CoAl, and NiAl using the self-consistent APW method. However, they published only the results for CoAl. *Ziesche* et al.[6] calculated the band structure of FeAl non self-consistently by the H-NFE-TB method. Furthermore *Müller* et al.[7] used the same method for the non self-consistent calculation of band structures and the interpretation of soft X-ray emission spectra of VAl, CrAl, FeAl, CoAl, and NiAl. *Hackenbracht* and *Kübler*[8] performed a calculation of the electronic structure and the cohesive properties of NiAl and Ni_3Al by means of the ASW method developed by *Williams* et al.[9]. Also "Scattered Wave" Xα-calculations on transition metal-aluminium clusters were performed by *Weinberger*[10] and *Müller* et al.[11].

Computational Aspects

The band structures, reported in this paper, were calculated self-consistently using the non-relativistic APW method[12, 13]. In the self-consistency procedure the muffin tin approximation was applied to the crystal potential as well as to the charge density. The exchange potential was treated by the Xα-method using the optimized atomic α-values as calculated by *Schwarz*[14] inside the atomic spheres and an α-value of 2/3 for the region of constant potential between the atomic spheres (see Table 1).

The starting potential for the band structure calculations was constructed by superposing the *Hartree-Fock-Slater* (*HFS*) Xα-potentials of the constituent atoms in their ground states[15]. In the present calculation the transition metal atom is located at the origin of the unit

cell and the aluminium atom is placed on the site $a\left(\frac{1}{2},\frac{1}{2},\frac{1}{2}\right)$. The atomic sphere radii R_M and R_{Al} were determined by the intersection of the superposed atomic *HFS*-Xα-potentials in the [111] direction (see Table 1) and were kept constant during the self-consistency procedure. The aluminium "1 s", and "2 s" and the transition metal "1 s", "2 s", "2 p", and "3 s" states were assumed to be core states for which the frozen core approximation was used, i.e. the self-consistent atomic *HFS*-Xα-charge densities were taken.

Table 1. *Input parameters for the APW band structure calculations*

Compound MAl	Exchange parameters α_M	α_{Al}	Lattice constant Å	(a.u.)	Atomic sphere radii R_M	R_{Al}
FeAl	0.71094	0.72795	2.908586	5.496190	2.365461	2.394379
CoAl	0.70966	0.72795	2.862482	5.409070	2.315721	2.368671
NiAl	0.70843	0.72795	2.886524	5.454500	2.318545	2.405190

The expansion of the APW wave functions inside the atomic spheres was carried up to a maximum l value of 12 and the variational expansion of the total crystal wave function in terms of augmented plane waves included reciprocal lattice vectors $\vec{\mathrm{k}}_i$ up to $|\vec{\mathrm{k}}_i| = |\vec{\mathrm{k}} + \vec{\mathrm{K}}_i| = 3.2\left(\frac{2\pi}{a}\right)$.

Energy eigenvalues and wave functions were obtained for 35 non-equivalent $\vec{\mathrm{k}}$ points in 1/48 of the *BZ*. These 35 points correspond to 512 uniformly distributed grid points in the whole *Brillouin* zone (*BZ*).

About 12 iterations were performed in order to obtain a difference of about 0.002 Ryd between the energy eigenvalues of the two last iterations. Further computational details are given by *Pechter*[16].

Results and Discussion

1. Band Structure

In Table 2 the self-consistent energy eigenvalues $E_\mu(\vec{\mathrm{k}})$ of CoAl with respect to the constant potential between the atomic spheres and the partial charges $q_l^t\left(E_{\vec{\mathrm{k}}}^{\mu}\right)$ and $q^{out}\left(E_{\vec{\mathrm{k}}}^{\mu}\right)$ are listed for the valence states corresponding to a coarse grid of 10 non-equivalent points in the irreducible wedge of the *BZ*. Using the standard notation of *Bouckaert*,

Table 2. *Partial charges* $q_l^t(E_\mu(\vec{k}))$ *and* $q_{out}(E_\mu(\vec{k}))$ *(in per cent) for the states* $E_\mu(\vec{k})$ *(in Ryd) of* CoAl

State $\vec{k}$	μ	$E_\mu(\vec{k})$	Co-sphere $l=0$	$l=1$	$l=2$	$l=3$	total	Al-sphere $l=0$	$l=1$	$l=2$	$l=3$	total	$q_{out}(E_\mu)$
000	Γ_1	−0.06925	25.29	0.00	0.00	0.00	25.291	40.28	0.00	0.00	0.00	40.284	34.425
		1.80392	40.18	0.00	0.00	0.00	41.723	43.79	0.00	0.00	0.00	45.148	13.129
	Γ_{12}	0.49348	0.00	0.00	81.45	0.00	81.453	0.00	0.00	4.39	0.00	4.569	13.978
		1.36184	0.00	0.00	27.02	0.00	27.599	0.00	0.00	37.13	0.00	37.140	35.261
	$\Gamma_{25'}$	0.64737	0.00	0.00	96.56	0.00	96.579	0.00	0.00	1.25	0.00	1.579	1.842
	Γ_{15}	1.16451	0.00	21.59	0.00	3.33	24.953	0.00	47.52	0.00	2.92	50.459	24.588
444	R_1	1.42166	75.63	0.00	0.00	0.00	75.964	0.00	0.00	0.00	8.88	8.876	15.159
	$R_{2'}$	1.00397	0.00	0.00	0.00	5.15	5.152	84.53	0.00	0.00	0.00	84.770	10.078
	R_{12}	0.68870	0.00	0.00	98.82	0.00	98.833	0.00	0.00	0.00	0.00	0.096	1.071
	R_{15}	0.90914	0.00	36.21	0.00	0.71	36.941	0.00	0.00	22.76	0.00	22.896	40.163
	$R_{25'}$	0.43465	0.00	0.00	63.87	0.00	63.890	0.00	19.23	0.00	0.11	19.393	16.717
		1.09896	0.00	0.00	44.66	0.00	44.708	0.00	35.16	0.00	1.16	36.351	18.941
440	M_1	0.49490	11.25	0.00	63.75	0.00	75.024	0.00	0.00	6.71	0.00	6.820	18.155
		0.90768	33.29	0.00	35.86	0.00	69.230	0.00	0.00	13.21	0.00	13.359	17.411
	M_3	0.34061	0.00	0.00	47.60	0.00	47.601	30.50	0.00	3.12	0.00	33.686	18.713
		0.95483	0.00	0.00	58.41	0.00	58.437	31.42	0.00	1.99	0.00	33.550	8.013
	M_2	0.68620	0.00	0.00	98.64	0.00	98.652	0.00	0.00	0.00	0.00	0.131	1.216
	$M_{2'}$	1.63312	0.00	0.00	0.00	7.21	7.394	0.00	79.90	0.00	0.54	80.529	12.076
	M_5	0.60207	0.00	0.00	92.15	0.00	92.189	0.00	0.00	3.25	0.00	3.418	4.393
	$M_{5'}$	0.53775	0.00	22.43	0.00	0.57	23.002	0.00	38.59	0.00	0.52	39.111	37.887
400	X_1	0.25291	26.05	0.00	12.63	0.00	38.688	0.00	27.10	0.00	0.01	27.119	34.193
		0.72037	5.36	0.00	86.58	0.00	91.985	0.00	4.06	0.00	0.18	4.310	3.704
	X_3	0.65512	0.00	0.00	97.42	0.00	97.425	0.00	0.00	0.00	0.89	0.937	1.637
	$X_{3'}$	1.34566	0.00	0.00	0.00	7.63	7.659	0.00	0.00	48.42	0.00	48.499	43.842
	X_2	0.53340	0.00	0.00	88.71	0.00	88.729	0.00	0.00	0.00	1.33	1.342	9.929
	$X_{4'}$	0.23616	0.00	17.26	0.00	0.12	17.381	47.14	0.00	2.68	0.00	49.822	32.797
		1.78670	0.00	16.77	0.00	8.85	25.728	31.37	0.00	12.10	0.00	44.932	29.340
	X_5	0.58740	0.00	0.00	89.39	0.00	89.448	0.00	4.68	0.00	0.83	5.560	4.993
		1.55579	0.00	0.00	19.39	0.00	20.301	0.00	62.36	0.00	1.45	63.863	15.836
	$X_{5'}$	1.51401	0.00	31.13	0.00	4.35	35.539	0.00	0.00	35.86	0.00	36.715	27.746

442	T_1	0.57528	5.33	3.41	71.65	0.17	80.561	0.00	0.00	5.21	0.02	5.362	14.078
		0.91067	24.98	8.79	27.80	0.14	61.765	0.00	0.00	15.18	0.26	15.489	22.746
		1.68935	38.77	28.56	1.44	0.01	69.078	0.00	0.00	2.27	8.89	11.668	19.254
	T_2	0.68735	0.00	0.00	98.73	0.00	98.747	0.00	0.00	0.00	0.00	0.113	1.140
	$T_{2'}$	0.68279	0.00	0.00	53.60	0.07	53.667	18.24	8.41	1.61	0.07	28.389	17.944
		0.96604	0.00	0.00	46.91	0.89	47.821	40.70	1.31	0.91	0.35	43.334	8.845
		1.31284	0.00	0.00	7.39	4.34	12.036	21.07	45.33	3.18	0.08	69.973	17.991
	T_5	0.46716	0.00	4.92	52.59	0.18	57.710	0.00	21.98	0.04	0.13	22.237	20.053
		0.73625	0.00	18.80	34.86	0.22	53.919	0.00	13.21	7.46	0.32	21.032	25.048
		1.38411	0.00	11.25	20.36	1.78	33.481	0.00	17.12	16.04	2.34	35.657	30.862
422	S_1	0.39949	13.40	7.40	19.82	0.17	40.799	0.00	26.28	1.33	0.07	27.718	31.483
		0.60056	2.73	0.33	85.54	0.17	88.785	0.00	0.06	3.97	0.09	4.230	6.986
		0.72759	5.24	1.63	81.74	0.01	88.648	0.00	4.25	1.35	0.02	5.730	5.622
		1.27962	24.61	2.22	13.24	2.04	42.197	0.00	16.87	13.06	2.85	32.851	24.952
	S_2	0.50604	0.00	0.00	73.88	0.22	74.112	0.00	12.03	1.60	0.08	13.794	12.093
		1.15185	0.00	0.00	32.02	1.48	33.521	0.00	32.95	8.40	0.62	42.037	24.442
	S_3	0.32363	0.00	9.00	23.67	0.08	32.754	31.03	8.24	1.14	0.21	40.652	26.594
		0.66868	0.00	9.85	63.20	0.04	73.131	2.11	6.04	4.19	0.35	12.755	14.114
		1.19457	0.00	8.12	12.89	2.44	23.725	40.47	15.41	2.59	0.83	59.424	16.851
		1.66392	0.00	6.88	7.99	5.08	20.348	2.17	29.76	19.66	1.64	53.690	25.962
	S_4	0.58093	0.00	2.57	85.15	0.10	87.830	0.00	0.00	1.83	0.52	2.465	9.705
		1.17385	0.00	30.00	15.79	0.10	46.021	0.00	0.00	21.76	0.98	22.849	31.130
420	Z_1	0.33455	20.97	4.23	13.84	0.11	39.156	0.00	25.66	1.52	0.01	27.201	33.642
		0.55051	0.02	2.20	82.95	0.04	85.226	0.00	1.45	1.08	0.88	3.477	11.297
		0.71585	3.49	0.93	86.67	0.04	91.162	0.00	4.52	0.05	0.05	4.750	4.089
		1.14439	17.92	14.52	12.37	1.21	46.098	0.00	6.41	19.27	0.94	26.792	27.111
	Z_2	0.59462	0.00	0.00	90.72	0.01	90.775	0.00	2.40	1.60	0.42	4.523	4.702
		1.58374	0.00	0.00	13.25	2.28	16.195	0.00	66.54	1.12	0.96	68.770	15.035
	Z_4	0.62695	0.00	0.08	94.31	0.05	94.461	0.00	0.00	1.85	0.39	2.353	3.186
		1.64173	0.00	27.28	6.99	2.74	37.343	0.00	0.00	34.58	1.26	36.556	26.101
	Z_3	0.28056	0.00	12.18	13.18	0.07	25.430	40.16	2.98	2.13	0.13	45.402	29.168
		0.56588	0.00	6.31	61.30	0.27	67.913	0.31	14.15	1.50	0.40	16.436	15.651
		1.11235	0.00	2.10	30.18	1.58	33.907	15.23	20.14	8.87	0.12	44.474	21.620
		1.63609	0.00	8.30	0.49	6.25	15.744	17.47	0.45	28.86	3.29	50.301	33.954

Table 2 (continued)

State			Co-sphere					Al-sphere					$q_{out}(E_\mu)$
$\vec{k}$	μ	$E_\mu(\vec{k})$	$l=0$	$l=1$	$l=2$	$l=3$	total	$l=0$	$l=1$	$l=2$	$l=3$	total	
222	Λ_1	0.16878	14.15	7.42	4.03	0.01	25.620	30.77	9.89	0.39	0.08	41.132	33.248
		0.58885	5.28	0.25	77.37	0.26	83.170	1.24	3.70	2.45	0.60	8.044	8.786
		1.07858	18.12	0.96	19.55	1.80	40.501	30.67	5.84	5.02	1.53	43.092	16.407
		1.60975	12.10	7.67	0.02	3.96	24.461	9.13	35.38	13.08	1.16	59.186	16.353
	Λ_3	0.50953	0.00	4.09	64.56	0.18	68.845	0.00	11.67	2.36	0.09	14.233	16.922
		0.59406	0.00	0.62	90.09	0.14	90.857	0.00	0.61	1.74	0.44	2.880	6.263
		0.93656	0.00	13.36	36.03	0.37	49.819	0.00	22.04	6.45	0.13	28.727	21.454
		1.51588	0.00	13.47	15.04	2.41	31.205	0.00	8.64	24.36	3.06	36.215	32.580
220	Σ_1	0.09453	18.03	5.55	1.43	0.01	25.015	33.68	6.93	0.36	0.02	40.995	33.990
		0.49162	2.46	1.09	69.25	0.12	72.936	3.04	4.84	3.15	0.30	11.423	15.641
		0.58100	0.86	0.34	86.42	0.17	87.796	0.29	3.52	0.43	0.78	5.094	7.110
		0.96916	12.63	4.80	31.12	0.98	49.538	15.26	9.68	7.29	0.38	32.758	17.704
		1.41631	8.75	4.48	5.45	4.65	23.583	0.26	7.32	32.35	2.08	42.097	34.320
		1.60953	0.28	9.02	17.94	1.24	29.044	15.95	6.51	17.42	2.68	42.709	28.247
	Σ_2	0.62478	0.00	0.00	94.33	0.04	94.388	0.00	0.00	2.16	0.12	2.481	3.131
	Σ_3	0.61696	0.00	0.22	92.00	0.07	92.317	0.00	2.87	0.21	0.73	3.909	3.774
		1.87129	0.00	17.19	8.89	2.20	28.601	0.00	40.85	7.08	1.78	49.951	21.449
	Σ_4	0.50608	0.00	6.93	58.12	0.09	65.161	0.00	11.01	2.94	0.26	14.263	20.575
		0.84130	0.00	12.18	39.87	0.64	52.726	0.00	25.11	2.64	0.09	27.980	19.294
200	Δ_1	0.01484	21.78	3.01	0.25	0.01	25.046	36.51	3.99	0.10	0.00	40.599	34.355
		0.46855	1.48	5.24	56.07	0.02	62.826	3.07	8.37	4.17	0.10	15.704	21.471
		0.83077	6.70	7.89	39.49	0.86	54.954	6.43	19.37	1.76	0.54	28.186	16.860
		1.62116	12.87	0.21	9.21	3.06	26.047	17.82	0.10	22.87	3.29	44.304	29.649
	Δ_2	0.51264	0.00	0.00	84.72	0.03	84.751	0.00	0.00	2.38	0.63	3.112	12.137
		1.35497	0.00	0.00	15.32	3.32	18.992	0.00	0.00	42.05	0.00	42.096	38.911
	$\Delta_{2'}$	0.65114	0.00	0.00	96.99	0.00	97.002	0.00	0.00	0.63	0.44	1.261	1.736
	Δ_5	0.61477	0.00	0.15	91.98	0.06	92.216	0.00	2.93	0.47	0.49	4.053	3.731
		1.27228	0.00	20.21	4.93	2.78	28.091	0.00	40.79	5.85	1.93	48.769	23.140

Smoluchovski, and *Wigner*[17], μ denotes the irreducible representation of the point group of the group of the wave vector $\vec{k}$. $q_l^t\left(E_{\vec{k}}^{\mu}\right)$ is the partial charge associated with the angular momentum quantum number l inside the atomic sphere t and $q^{out}\left(E_{\vec{k}}^{\mu}\right)$ is the charge in the unit cell between the atomic spheres for a particular state with the energy eigenvalue $E_{\vec{k}}^{\mu}$. The charges are normalized to 1 in the unit cell

$$\sum_{t=1}^{n} \sum_{l=0}^{12} q_l^t\left(E_{\vec{k}}^{\mu}\right) + q^{out}\left(E_{\vec{k}}^{\mu}\right) = 1. \tag{1}$$

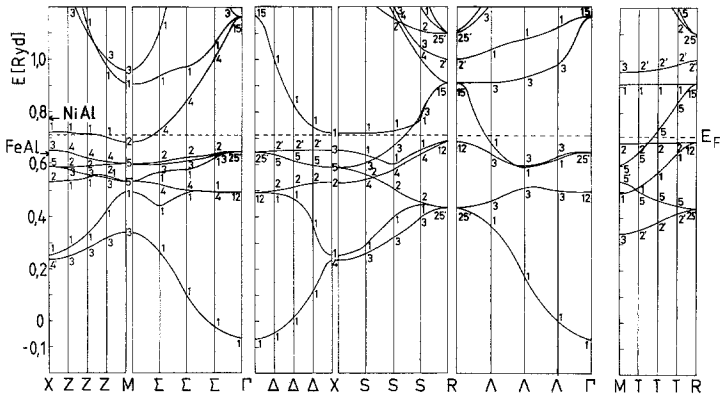

Fig. 1. APW band structure of CoAl in six symmetry directions (energies with respect to the muffin tin zero). The arrows labeled by "FeAl" and "NiAl" indicate the *Fermi* energy $E_{F'}$ for FeAl and NiAl relative to the position of the d-bands of these compounds. $E_{F'}$ is calculated according to $E_{F'}^{M\mathrm{Al}} = E_F^{M\mathrm{Al}} - E_{\Gamma_{25'}}^{M\mathrm{Al}} + E_{\Gamma_{25'}}^{\mathrm{CoAl}}$ $(M = \mathrm{Ni}, \mathrm{Fe})$

A complete description of the evaluation of the partial charges is given by *Neckel* et al.[13].

The electronic energy bands of CoAl along the six $\vec{k}$-directions which enclose the irreducible wedge of the *BZ* are shown in Fig. 1. The band structures of FeAl and NiAl exhibit a largely similar behaviour, except for the d-band width, which decreases from FeAl to NiAl (see Table 3), and of course the *Fermi* level (Table 3) whose position for the two other compounds is marked by an arrow in Fig. 1.

The state $E(\Gamma_1)$ in the lowest energy band of the valence states possesses pure s-character (see Table 2). Around the state $E(\Gamma_1)$ the surfaces of constant energy are largely spherical and the $\vec{k}$-dependence of the energy is approximately parabolic, corresponding to the behaviour of a nearly free electron gas. This nearly free electron character near the bottom of the band is primarily due to the relatively high position of the d-bands. The broad quasi free electron band, which can be regarded as the Al s-band, is intersected in its upper region by a set

Table 3. *Fermi energy with respect to the constant muffin tin potential and energy difference* $E_{R_{25'}} - E_{X_1}$ *as a measure of d-band width (in Ryd)*

	FeAl	CoAl	NiAl
E_F	0.6574	0.7125	0.6859
$R_{25'}$—X_1	0.3120	0.2862	0.2362

of d-bands which originate in the points $E(\Gamma_{12})$ and $E(\Gamma_{25'})$. The wave functions of these two states possess pure d-character and are almost exclusively located within the transition metal sphere [Charges inside the transition metal sphere are for $E(\Gamma_{12}) \sim 81.5\%$, $E(\Gamma_{25'}) \sim 96.5\%$]. The charges of other symmetry points with prevailing d-character (e.g. X_5, X_3) are also mainly localised inside the transition metal sphere.

In the lower energy range the transition metal d-functions hybridize strongly with s- and p-functions of both, the transition metal and aluminium atom. For example the energy state of $E(X_1)$ contains, besides a small contribution of transition metal d-character (13%), transition metal s- (26%) and aluminium p-character (27%). In a similar way also the wave functions of the d-bands in the upper energy region are hybridized. For example, in the energy band originating at $E(\Gamma_{25'})$ the d-character in the transition metal sphere decreases along the Λ_1 direction towards $E(R_{15})$ while the p-character in the aluminium sphere increases. The state $E(R_{15})$ possesses about 37% transition metal d-character and about 22% aluminium p-character. The width of the d-band decreases going from FeAl to NiAl as can be seen from the difference $[E(R_{25'})\text{-}E(X_1)]$ in Table 3. Comparing the partial charges of special energy states $E_\mu(\vec{k})$ for the three compounds a large agreement is found.

Comparison with Other Band Structure Calculations

Connolly and *Johnson*[2] calculated the band structure of NiAl non self-consistently using both the APW and the KKR method. The crystal potential was generated by the superposition of the neutral atomic charge densities

derived from the electronic configuration Al: $(3s)^2(3p)^1$ and Ni: $(3d)^9(4s)^1$. The full *Slater* exchange potential ($\alpha = 1$) was used. The results of the APW and KKR calculation of these authors agree within a few mRyd. Although *Connolly* and *Johnson* used an α-parameter of unity and atomic sphere radii ($R_{Ni} = 2.622$ a.u.; $R_{Al} = 2.451$ a.u.) differing from those of the present calculation (Table 1), their results agree fairly well with the results presented in this paper. The largest deviation between the two sets of energy values (taken with respect to the *Fermi* energy) amounts to ± 0.03 Ryd. A detailed comparison of the two calculations shows that in the present self-consistent APW calculation the energies of the strongly localised states are lowered with respect to the non-self-consistent energies, whereas the mainly delocalised states remain energetically constant.

The self-consistent KKR calculations of *Moruzzi*, *Janak*, and *Williams*[3] on NiAl and CoAl agree very well with the present self-consistent APW results, although these authors use for both compounds and for both atomic spheres the same α-parameters ($\alpha = 0.77$), and equal muffin-tin spheres. In general the deviations of the energy eigenvalues (referred to equal *Fermi* energy) between the two calculations amount to a few mRyd. The maximum difference for NiAl is 14 mRyd, for CoAl 12 mRyd. These differences show the order of magnitude of the influence of the exchange parameters and of the atomic sphere radii.

The non self-consistent band structure of FeAl obtained by *Okochi*[4] using the APW method differs appreciably from the self-consistent band structure of the present paper. For example the energy $E(\Gamma_1)$ in *Okochi*'s calculation lies about 0.2 Ryd higher than the present one. Furthermore the sequence of the energy eigenvalues at the k-points X and M is changed, so that different compatibilities result. The width of the d-band is much smaller [$(E(R_{25}) - E(X_1) = 0.2341$ Ryd]. The differences between these two bandstructures can be attributed not only to the use of different exchange parameters ($\alpha = 1$)[4] but mainly to the fact that the superposed crystal potential which *Okochi* used, had been derived from the electronic configuration Al: $(3s)^2(3p)^1$ and Fe: $(3d)^6(4s)^2$. The charge distribution in the crystal, however, does not correspond to this electron configuration of the iron atom, as will be seen from the charge analysis of the self-consistent APW calculation given below (Table 4).

Ziesche et al.[6] performed a non self-consistent band structure calculation for FeAl by means of the "Hybridized Nearly Free Electron-Tight Binding" (H-NFE-TB) method. The crystal potential was constructed by the superposition of the atomic potentials derived from the electronic configuration Al: $(3s)^2(2p)^1$ and Fe: $(3d)^7(4s)^1$. The band structure, calculated by these authors, agrees much closer with the results of the present paper than with the band structure of *Okochi*, although significant differences remain. Thus the state $E(\Gamma_1)$ is found to lie about 0.85 Ryd below the *Fermi* energy, in constrast to 0.72 Ryd in the present paper.

Recently *Müller* et al.[7] published band structures of five transition metal aluminides calculated by the same method. Their results for FeAl, CoAl, and NiAl agree fairly well with our band structures, especially in the d-band width which, measured by the distance $E(R_{25'})$-$E(X_1)$, is practically the same in both calculations. However there remain some minor differences regarding the position of the bottom of the s-band with respect to the *Fermi* level.

In comparison to our results the density of states curve reported by *Hackenbracht* and *Kübler*[8] for NiAl seems to indicate a slightly larger d-band width. These authors obtain a qualitatively very similar charge distribution in the crystal. A quantitative comparison is, however, not possible, since they use space

filling (overlapping) atomic spheres. Consequently their partial charges and local partial densities of states are always higher, since they refer to atomic spheres which are larger than the muffin tin spheres used in the present APW calculations. In the latter almost two electrons reside in the region outside the muffin tin spheres which are included in the partial local charges of Ref.[8].

Nagel et al.[5] report on self-consistent APW band structure calculations on FeAl, CoAl, and NiAl. However, only the band structure of CoAl and its partial densities of states are displayed in the paper and no energy values are given. As far as can be judged from the figure given in their paper their band structure of CoAl is in good agreement with the present one.

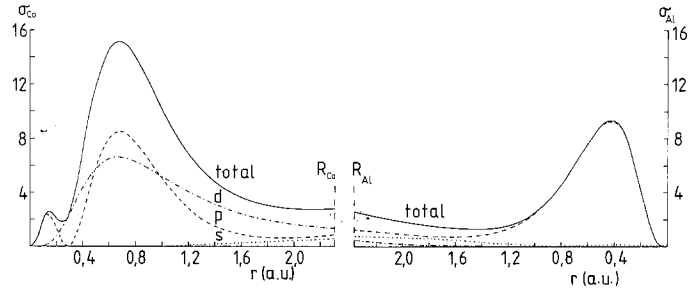

Fig. 2. Radial charge densities $\sigma^t(r)$ of the semicore and valence states of CoAl inside the Co sphere (left side) and the Al sphere (right side): ———— total radial charge density $\sigma^t(r)$; ····· partial s-charge density $\sigma_s^t(r)$; — — — — — partial p-charge density $\sigma_p^t(r)$; —·—·—· partial d-charge density $\sigma_d^t(r)$; R_{Al} and R_{Co} are the muffin tin radii

2. *Charge Distribution*

In order to get an insight into the charge distribution in the crystals, the radial charge densities $\sigma_l^t(r) = 4\pi r^2 \rho_l^t(r)$ summed over all occupied semi-core and valence states are shown for CoAl as a representative example in Fig. 2 ($\rho_l^t(r)$ is the l-component of the spherically averaged electron density in the atomic sphere t at a distance r from the origin of that sphere). In the aluminium sphere the radial charge density consists mainly of the aluminium 3 p component, while in the transition metal-sphere the 3 d component dominates.

By radial integration of $\sigma_l^t(r)$ up to the atomic sphere radius R_t, the partial local charges Q_l^t of the semi-core and valence states inside the atomic sphere t are obtained as well as the charge q^{out} in the region of constant potential between the atomic spheres (Table 4).

3. *Charge Transfer*

In order to evaluate the charge transfer in the crystal an appropriate reference state must be chosen. *Moruzzi* et al.[3] used as reference

Table 4. *APW charge analysis of* FeAl, CoAl, *and* NiAl *as defined by Neckel et al.*[13]: *Partial charges* (Q_{nl}^t) *inside atomic sphere t, charge outside the muffin tin spheres* q^{out} *and atomic superposed charge* $Q_{at.s}$ *are given in number of electrons per unit cell*

	NiAl	CoAl	FeAl
Transition metal-sphere M	Ni	Co	Fe
core ($1s^2\ 2s^2\ 2p^6\ 3s^2$):	12.000	11.999	11.999
semi-core: 3p	5.993	5.988	5.985
valence: 3d	8.050	7.575	6.481
4d	0.435	0.000	0.000
4s	0.415	0.373	0.364
4p	0.444	0.411	0.403
higher nl	0.019	0.015	0.015
total: $Q^M_{crystal}$	27.356	26.361	25.247
atomic superposed: $Q^M_{at.s.}$	27.160	26.115	25.094
$Q^M_{crystal} - Q^M_{at.s.}$	0.196	0.246	0.153
Al-sphere	Al	Al	Al
core: ($1s^2\ 2s^2$)	4.000	4.000	4.000
semi-core: 2p	5.997	5.997	5.997
valence: 3s	0.693	0.685	0.713
3p	0.882	0.850	0.894
3d	0.194	0.208	0.209
higher nl	0.051	0.048	0.045
total: $Q^{Al}_{crystal}$	11.817	11.788	11.858
atomic superposed: $Q^{Al}_{at.s.}$	12.084	12.073	12.095
$Q^{Al}_{crystal} - Q^{Al}_{at.s.}$	−0.267	−0.285	−0.237
Region outside atomic spheres			
APW: $q^{out}_{crystal}$	1.827	1.851	1.894
atomic superposed: $q^{out}_{at.s.}$	1.756	1.812	1.811
$q^{out}_{crystal} - q^{out}_{at.s.}$	0.071	0.039	0.083

the pure metal, crystallizing in the same crystal structure as the compound. Thus, for instance, they compared the radial charge density inside the nickel sphere of NiAl with that of nickel crystallizing in the *bcc* structure with the lattice spacings of NiAl.

In the present paper a different reference state is taken. The charge density in the crystal is supposed to be formed in two steps: in the first step neutral atoms with valence electron configurations Al: $(3s)^2\,(3p)^1$ and transition metal: $(3d)^n\,(4s)^1$ ($n = 7, 8, 9$ for Fe, Co, Ni) are placed

on the lattice sites of the ordered compound and their atomic charge densities are superposed. The resulting charge distribution forms our reference state for the charge transfer and would be the basis of a non self-consistent calculation.

In the second step the electron density is redistributed self-consistently leading to the charge distribution of the real crystal. This charge redistribution and the corresponding charge transfer represent the effect of the self-consistency procedure. Charge transfers given by

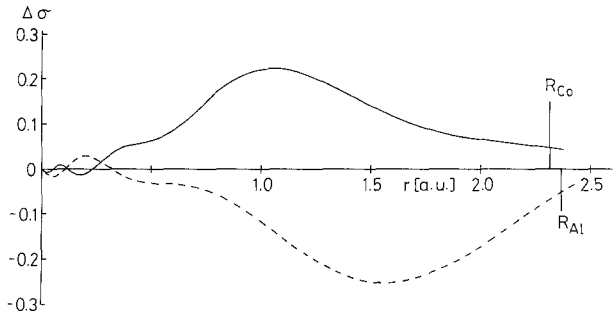

Fig. 3*a*. Charge transfer $\Delta\sigma^t(r)$ of CoAl in terms of the difference $\Delta\sigma^t(r) = \sigma^t(r) - \sigma^{t,sup.at.}(r)$ of the self-consistent APW charge density $\sigma^t(r)$ and the atomic superposed charge density $\sigma^{t,at.sup.}(r)$ calculated using the electron configuration Co: $3d^8\,4s^1$. Full curve: Co sphere; broken curve: Al sphere

other authors are defined differently[18] and consequently quantitative comparisons are rather difficult to be made.

The difference $\Delta\sigma^t(r) = \sigma^t(r) - \sigma^{t,sup.at.}(r)$ of the radial charge densities between the compound, $\sigma^t(r)$, and the hypothetical crystal of the superposed atoms, $\sigma^{t,sup.at.}(r)$, plotted versus the distance r from the origin of the atomic sphere t is displayed for CoAl in Fig. 3*a*. From this figure it can be seen that in the real crystal the electron density has increased in the transition metal sphere (full curve)—except for a small range near the nucleus—while it has decreased in the aluminium sphere (dashed curve) in comparison to the hypothetical crystal of superposed atomic charges.

Although *Moruzzi* et al.[3] use a different reference state, their results are qualitatively similar. They also obtain an increase of the electronic charge density in the nickel and cobalt sphere (FeAl was not investigated) and—following a small maximum—a decrease of the electron density in the aluminium sphere. The dependence of $\Delta\sigma^t(r)$ on

the distance r from the nucleus, however, is different. In their calculation $\Delta\sigma^t(r)$ is monotonically increasing in the nickel and cobalt sphere and monotonically decreasing in the aluminium sphere.

Our reference state corresponds to the transition metal configuration $(3\,d)^n(4\,s)^1$ rather than to the atomic ground state configuration $(3\,d)^{n-1}(4\,s)^2$. Assuming these two configurations Fig. 3*b* shows the difference of the corresponding superposed atomic charge densities. Promoting one of the largely delocalised 4 s electrons into the more localised 3 d state, results in a reduction of the charge density inside the

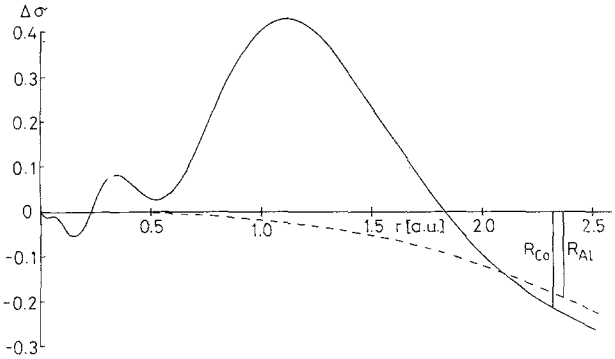

Fig. 3*b*. The effect of the atomic Co configuration on the atomic superposed charge densities is shown in form of $\Delta\sigma^{t,at.\,sup.}(r) = \sigma^{t,at.\,sup.}(r)$ [Co: $3d^8\,4s^1$]— —$\sigma^{t,at.\,sup.}(r)$ [Co: $3d^7\,4s^2$]. Full curve: Co sphere; broken curve: Al sphere

aluminium sphere. Inside the cobalt sphere this promotion has the effect of contracting the charge density and increasing the total charge; the negative part of $\Delta\sigma$ at large radii is mainly due to the reduced number of s-electrons.

If the ground state configuration would have been used for the reference state, the two effects as shown in Figs. 3*a* and 3*b* would add up, resulting in a much larger charge transfer. In the case of the cobalt sphere the atomic configuration has a much larger effect on the charge distribution than the self-consistency procedure. A further increase in the number of 3 d electrons could reproduce the crystal charge density inside the cobalt sphere even better. Since in the aluminium sphere the $\Delta\sigma$ curves shown in Fig. 3*a* and 3*b* have a different radial dependence, it can be concluded that its radial charge density is not so much affected by the cobalt configuration as by the self-consistency effects.

Fig. 3*b* also explains why *Okochi*'s energy bands of FeAl based on the $(4\,s)^2$ configuration deviate significantly from the self-consistent results.

A comparison of the charges inside the atomic spheres in the real crystal with the charges inside the atomic spheres of the hypothetical crystal of superposed atomic charges (Table 4) reveals that in the real crystal the charges in the transition metal spheres have increased by about 0.15 to 0.25 electrons, the charges in the aluminium spheres have decreased by about 0.25 electrons, while the charge between the atomic spheres has been slightly raised (0.04 to 0.08 electrons). It should be noted that the presence of neighbouring transition metal atoms leads to the appearance of electrons with d-symmetry (about 0.2 electrons) in the aluminium sphere (Table 4).

4. *Knight Shift*

The *Fermi* level falls in FeAl and CoAl within the d-bands, while for NiAl the *Fermi* energy lies above the d-bands. For FeAl the density of states at the *Fermi* level has nearly exclusively d-character, for CoAl and NiAl there are also contributions from states with other symmetry ($\sim 40\%$ for NiAl, $\sim 23\%$ for CoAl).

These results are in qualitative agreement with conclusions drawn from NMR measurements of FeAl, CoAl, and NiAl (see for example *Spokas* et al.[19]). The experiments show that the Al^{27} *Knight* shift is large and negative in FeAl and small and positive in NiAl and CoAl.

In general the main contribution to the *Knight* shift comes from the *Fermi* contact term, which is always positive and originates from the valence s-electrons at the *Fermi* energy, E_F. In transition metals and their compounds with partially filled d-bands a negative exchange term could also be important. This contribution comes from the polarization of the core s-electrons by uncoupled valence d-electrons.

The Al^{27} *Knight* shift experiments of the three compounds investigated suggest that the density of states (DOS) at E_F consists mainly of states with transition metal d-symmetry in the case FeAl (producing a large negative shift), whereas in CoAl and NiAl this component should be significantly smaller. This finding is consistent with the present calculation, according to which E_F falls in a region of high d DOS for FeAl, whereas in CoAl and NiAl the d DOS at E_F is much smaller.

5. *Fermi Surface*

The H-NFE-TB method was used to fit the APW energy eigenvalues[21]. With this scheme energy eigenvalues at 561 non equivalent $\vec{k}$ points were interpolated yielding a sufficiently fine grid to determine the intersection planes of the *Fermi* surface with the $\vec{k}_z = 0$ plane for FeAl, CoAl, and NiAl.

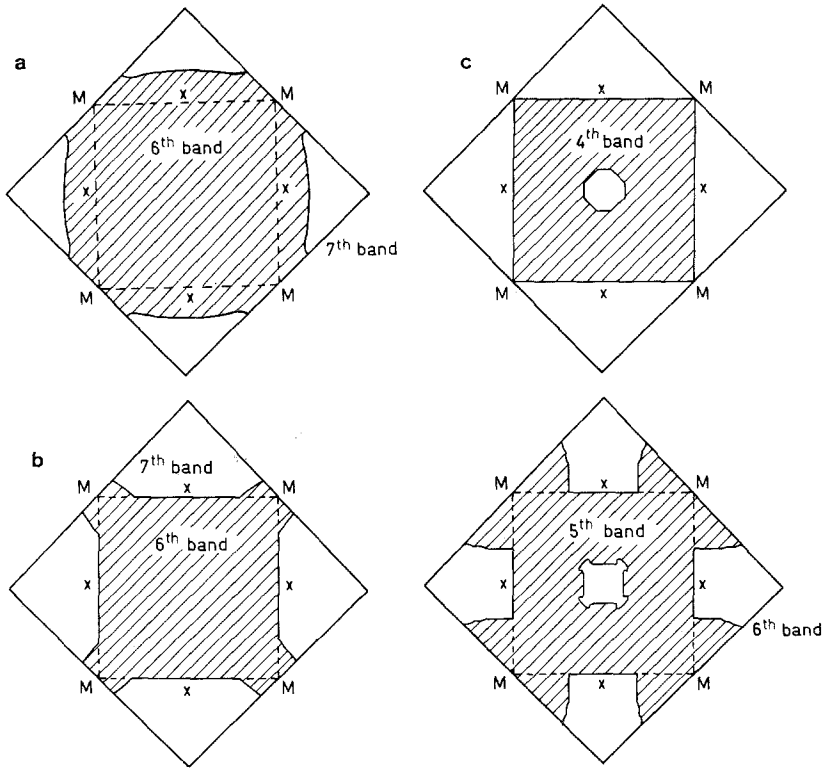

Fig. 4. Intersection of the *Fermi* surface of (*a*) NiAl, (*b*) CoAl, and (*c*) FeAl with the plane $k_z = 0$. For CoAl and NiAl the five filled d-bands are not shown. Only the sheets corresponding to the filled sixth and the partially filled seventh band are displayed. For FeAl three bands are filled. Fig. 4*c* shows only the hole sheets corresponding to the fourth and fifth and the electron sheet for the sixth band

If NiAl and CoAl could be treated as free electron-like *Hume-Rothery* phases with three valence electrons per unit cell, their first band (not counting the five occupied d-bands) should be full except for small isolated pockets of holes round the corners R of the *Brillouin* zone. Sheet 2 should consist of a multiple connected set of lenses centred at X so that a sphere touching the *Brillouin* zone at points M results.

Fig. 4*a*, however, shows that the *Fermi* sphere is slightly distorted and necks are formed around M for NiAl, whereas for CoAl only these necks remain occupied for the second band (Fig. 4*b*).

The *Fermi* surface of FeAl is more complicated because the *Fermi* level cuts the d-bands (Fig. 4*c*). There are holes around Γ in the sheets

corresponding to the fourth and fifth band which are totally occupied for NiAl and CoAl. The sheet corresponding to the sixth band shows large necks around M and pockets of holes in the S-direction ($X \rightarrow S \rightarrow R$). Unfortunately no direct measurements of the *Fermi* surface exist for the compounds in question.

The galvanomagnetic properties of NiAl have been explained[22] by assuming hole and electron conductivity in accordance with the present results. The hole contributions come from the region around the point R, not contained in the section of the *Fermi* surface shown in Fig. 4*a*.

6. *Further Experimental Properties*

The results of the self-consistent APW band structure calculations presented in this paper have been used to calculate various other physical properties of these crystals. Some of these properties require the knowledge of energy eigenvalues for a large number of $\vec{k}$ points in the *Brillouin* zone. Since in the present study the number of $\vec{k}$ points in the irreducible wedge of the first *Brillouin* zone (*BZ*) is restricted to 35, another paper[21] dealt with the interpolation of energy eigenvalues by applying a Hybridized-Nearly Free Electron-Tight Binding interpolation scheme. The results obtained were used to calculate the total and the partial densities of states, which were compared with experimental XPS- and UPS-spectra in the case of NiAl. Furthermore, the imaginary part of the complex dielectric function was calculated for the three compounds mentioned and compared with the experimental results for NiAl and CoAl. Based on the present APW calculations *Schwarz* et al.[20] calculated the soft X-ray emission spectra of FeAl and estimated the relative intensities of the Al-$L_{2,3}$- and the Fe-$M_{2,3}$-spectra. *Podloucky* and *Neckel*[23] used the APW wave functions of the present paper to calculate the *Compton* profiles for FeAl.

Acknowledgements

All computational work was performed at the "Interfakultäres Rechenzentrum der Universität Wien" whose assistance is gratefully acknowledged. This work was supported by the Austrian foundation "*Fonds zur Förderung der wissenschaftlichen Forschung*".

References

[1] *Hume-Rothery, W.*, in: Phase stability of Metals and Alloys (*Rudman, P., Stringer, J., Jaffée, J.*, eds.). New York: McGraw-Hill. 1967.
[2] *Connolly, J. W. D., Johnson, K. H.*, in: Electronic Density of States (*Bennett, L. H.*, ed.), pp. 19–25. NBS Spec. Publ. **323**, 1971.
[3] *Moruzzi, V. L., Williams, A. R., Janak, J. F.*, Phys. Rev. **B 10**, 4856 (1974).
[4] *Okochi, M.*, J. Phys. Soc. Jap. **B 9**, 367 (1975).

[5] *Nagel, D. J., Boyer, L. L., Papaconstantopoulos, D. A., Klein, B. M.*, In: Proc. Int. Conf. Trans. Metals (*Lee, M. G., Perz, M., Fawcett, E.*, eds.), p. 104. Toronto: 1977.
[6] *Ziesche, P., Wonn, H., Müller, Ch., Nemoshkalenko, V. V., Krivitskii, V. P.*, Phys. stat. solidi (b) **87**, 129 (1978).
[7] *Müller, Ch., Wonn, H., Blau, W., Ziesche, P., Krivitskii, V. P.*, Phys. stat. solidi (b) **95**, 215 (1979).
[8] *Hackenbracht, D., Kübler, J.*, J. Phys. **F** (Met. Phys.) **10**, 427 (1980).
[9] *Williams, A. R., Kübler, J., Gelatt, C. D.*, Phys. Rev. **B 19**, 6094 (1979).
[10] *Weinberger, P.*, Sol. State Phys. **10**, L 347 (1977).
[11] *Müller, Ch., Seifert, G., Lautenschläger, W., Wonn, H., Ziesche, P., Mrosan, E.*, Phys. stat. solidi (b) **91**, 605 (1979).
[12] *Mattheiss, L. F., Wood, J. H., Switendick, A. C.*, in: Methods in Computational Physics, Vol. 8, p. 63. New York: Academic Press. 1968.
[13] *Neckel, A., Rastl, P., Eibler, R., Weinberger, P., Schwarz, K.*, J. Phys. **C** (Sol. State Phys.) **9**, 579 (1976).
[14] *Schwarz, K.*, Phys. Rev. **B 5**, 2466 (1972).
[15] *Mattheiss, L. F.*, Phys. Rev. **133 A**, 1399 (1964).
[16] *Pechter, K.*, Thesis, University of Vienna, 1975.
[17] *Bouckaert, L. P., Smoluchowski, R., Wigner, E. P.*, Phys. Rev. **50**, 58 (1936).
[18] *Wenger, A., Bürri, G., Steinemann, S.*, Sol. State Comm. **9**, 1125 (1971).
[19] *Spokas, J. J., Sowers, C. H., Ostenburg, D. D. van, Hoeve, H. G.*, Phys. Rev. **B 1**, 2523 (1970).
[20] *Schwarz, K., Neckel, A., Nordgren, J.*, J. Phys. **F** (Met. Phys.) **9**, 2509 (1979).
[21] *Eibler, R., Neckel, A.*, J. Phys. **F** (Met. Phys.) **10**, 2179 (1980).
[22] *Yamaguchi, Y., Brittain, J. O.*, Phys. Rev. Letters **21**, 1447 (1968).
[23] *Podloucky, R., Neckel, A.*, Phys. stat. solidi (b) **95**, 541 (1979).